indicated in Fig. 3a a cratered lunar surface at subsolar conditions and at high observation angles (measured from the horizon) can be considered nearly Lamertian.

Figure 3b shows the directional behavior of brightness temperature for a 50° solar elevation (40° from zenith). The directionality is more pronounced here. It is interesting to note that the maximum of the brightness temperature is at a lower observation angle than the solar elevation angle. This behavior was also observed by Shorthill.[2] Furthermore, on the cool side, the crater with higher aspect ratio results in greater brightness temperature at low observation angles, despite the fact that the shadows of shallow craters are colder than those of deep craters. This apparent paradox can be explained by Fig. 2. By observing the shadowed side in a deep crater at a low observation angle, the warm region of the crater is not visible to the observer, while shallow craters are fully visible, including the sunlit region, which increases the average brightness temperature.

The directional behavior of the emission at 20° solar elevation is shown in Fig. 3c. The directionality is very pronounced, the maximum of the brightness temperature curve is lower than the solar elevation angle, especially at the higher aspect ratio crater, where it approaches the horizon. The point corresponding to the rough surface consisting of 90% flat plain and 10% $a = 3$ aspect ratio craters is also indicated on the hot side. The brightness temperature for such a surface is around 13° K higher than the brightness temperature of the Lamertian plan.

Figures 3a, b, and c well indicate that the lunar surface can be considered Lamertian at high solar elevation and observation angles. For low-solar elevation angles the surface deviates more and more from the Lambertian behavior. The present model is highly idealized, but a crater field still represents a reasonable approximation, as can be seen from the high resolution lunar photographs. Many of the lunar craters are flat bottomed and cannot be considered spherical. Such craters would increase the directionality even more at low-elevation angles.

In Fig. 4 the results of the present study are superimposed on the representation of experimental data given by Shorthill,[2] taken along the north and south sections of the lunar equator. The experimental data were approximated by two conditions, one is a $a = 7.5$ aspect ratio crater, the other is a mix of 10% $a = 3$, 20% $a = 4$, 30% $a = 7.5$ aspect ratio craters and 40% flat plain. Both of these hypothetical cases are in good agreement with the experimental data, both in magnitude and trend. In order to determine the directional behavior of the radiation in a particular region of the lunar surface, however, it is necessary to know the topography of that region.

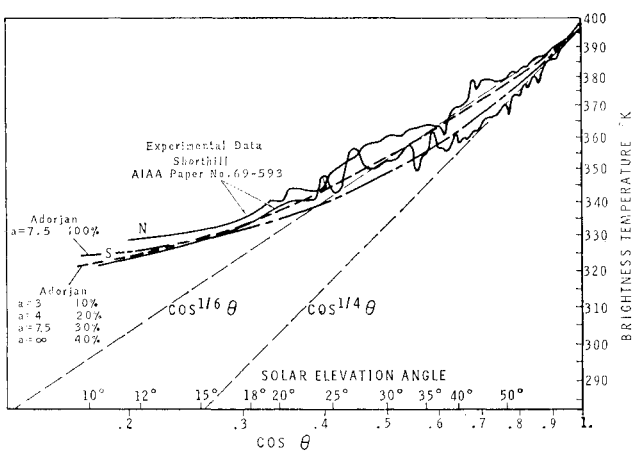

Fig. 4 Variation of brightness temperature of the full moon in north-south direction.

References

[1] Pettit, E., and Nicholson, B., "Lunar Radiation and Temperatures," *Astrophysical Journal*, Vol. 71, 1930, pp. 102–135.

[2] Shorthill, R. W., "The Infrared Moon," *Journal of Spacecraft and Rockets*, Vol. 7, No. 4, April 1970, pp. 385–397.

[3] Adorjan, A. S., "Temperature Distribution in Shadowed Lunar Craters," *Journal of Spacecraft and Rockets*, Vol. 7, No. 3, March 1970, pp. 378–380.

Exhaust Velocity Studies of a Solid Teflon Pulsed Plasma Thruster

KEITH I. THOMASSEN*
Massachusetts Institute of Technology, Cambridge, Mass.
AND
ROBERT J. VONDRA†
MIT, Lincoln Laboratory, Lexington, Mass.

Introduction

PULSED electric thrusters have proved to be useful for satellite control applications. We report here on a continuing diagnostics program on the solid Teflon fuel thrusters developed by Fairchild–Hiller[1] and used on the LES-6 satellite (Lincoln Experimental Satellites)[2,3]. The purpose of the program is to understand the physics of the discharge, develop mathematical models of the device to predict performance, and measure circuit and plasma parameters in order to improve the design and the efficiency of the thruster.

Our results to date have been summarized elsewhere.[4,5] Briefly, parameters for a simple RLC circuit model were determined and used to predict thruster efficiency and impulse bit. Langmuir probe and microwave interferometry determined plasma exhaust densities, a Faraday cup measurement of time-of-flight yielded exhaust ion velocities, and a thrust stand was built to measure impulse bit and specific impulse.

From the early results we found a mass averaged exhaust velocity $\bar{v} = 3000$ m/sec ($I_{SP} = 300$ sec), but a Faraday cup used to measure ion current yielded an ion velocity of 40,000 m/sec by a time-of-flight measurement. This prompted a more detailed investigation of the constituents in the exhaust, which we report here. We are interested in knowing the constituents in the exhaust and their velocities, first so that we might understand the plasma formation process better, and second in order to determine the kinetic energy in the exhaust. The latter determines the fraction of stored energy imparted to the exhaust while the former is important in considering the design changes which will improve this efficiency.

It is perhaps worthwhile to note that early estimates of the kinetic energy (2% of the initial stored energy) were in error because they assumed all components in the exhaust traveled at the mass-averaged velocity. On obtaining the Faraday cup measurements it was clear that the ionized portion of the exhaust was traveling much faster, hence that the total energy

Presented as Paper 71-194 at the AIAA 9th Aerospace Sciences Meeting, New York, January 25–27, 1971; Submitted March 1, 1971; revision received August 12, 1971. This work was sponsored by the Department of the Air Force.

Index category: Electric and Advanced Space Propulsion.

* Associate Professor, Electrical Engineering Department.

† Staff Member, Space Communications Division. Member AIAA.

$\sum_\alpha \frac{1}{2} m_\alpha v_\alpha^2$ (where α enumerates the various exhaust components) could differ greatly from the first estimate. The total momentum $\sum_\alpha m_\alpha v_\alpha$ and total mass $\sum_\alpha m_\alpha$ are available from thrust and mass measurements, but we need measurements of m_α and v_α for each component to correctly calculate the exhaust energy.

In this Note we report measurements of the velocities of the ions and excited neutrals, but not unexcited neutrals. The latter probably make up the largest fraction of the exhaust particles. A measurement of the charge in the exhaust using a Faraday cup indicates a maximum ionization percentage of 10%. From these data we obtain a better estimate of kinetic energy by assuming the neutrals (90% of the particles) have negligible velocities while the ions (the remaining 10%) travel with the "average ion velocity" $\simeq 30{,}000$ m/sec. By this crude partitioning we estimate the kinetic energy at 15% of the initial stored energy in the capacitor. Such a partitioning gives the correct exhaust momentum but is otherwise indefensible. Better estimates must await a mass analysis of the exhaust species, but even this preliminary calculation shows that considerable energy is given to a small fraction of the ions, resulting in a poor mass utilization. Similar "flow nonuniformity losses" have been reported[6] in an MPD arc, but the processes responsible for this energy partitioning in a gas filled region are considerably different than those occurring in our vacuum arc. Based on the spectroscopic studies reported here we can postulate a sequence of events leading to formation and acceleration of the exhaust plasma.

Spectroscopic Studies

We first made a complete survey of the lines observed in the plasma looking down the throat of the thruster with a 1-meter Jarrell Ash scanning spectrometer. Comparing the observed lines with a table[7] of lines of carbon and fluorine we identified all intense lines of neutral, (C_I, F_I), singly ionized (C_{II}, F_{II}), doubly ionized, and triply ionized atoms of each species in the range from 2100 Å–7300 Å, and thus were unable to look for more highly ionized species. The only other lines we could identify were numerous weak iron lines, coming apparently from bombardment of the stainless steel electrodes and spark plug erosion.

It is interesting to look at the time of formation of these lines. In Fig. 1 we show the photodiode output for F_I, F_{II}, F_{III}, F_{IV} along with a trace of the capacitor voltage waveform which decays in a damped oscillatory manner in a few microseconds. The species which require the most energy for creation reach their peak light intensity earliest. For doubly and triply ionized carbon and fluorine atoms this time is from 0.3–0.8 μsec, when the current in the discharge is greatest. Table 1 summarizes the data on formation and lifetimes of each type of ion, averaged over the several observed lines of each of the species.

There is evidence of recombination as can be seen from the observed 2479 Å and 2583 Å lines of C_I. The 2479 Å line peaks at 1.5 μsec and shows a neutral carbon velocity of

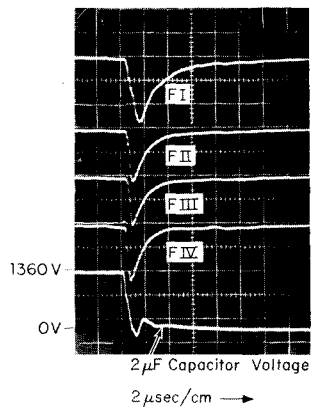

Fig. 1 Formation times of neutral (F_I), singly, doubly, and triply-ionized fluorine.

Table 1 Formation times and lifetimes of the various plasma species

Species	Peak luminosity time[a] (μsec)	Lifetime[b] (μsec)	Species	Peak luminosity time[a] (μsec)	Lifetime[b] (μsec)
CI	1.5	5.0	FI	1.3	4.0
CII	1.2	1.6	FII	0.8	1.2
CIII	0.8	1.2	FIII	0.5	1.0
CIV	0.3	0.5	FIV	0.3	0.4

[a] Time after initiation of discharge
[b] Time after discharge termination when luminosity is 10% of its peak value.

~ 6000 m/sec while the 2583 Å line peaks at 0.4 μsec and indicates a velocity of $\sim 18{,}000$ m/sec. This data is taken from later Doppler measurements which also show that the velocity of singly ionized carbon atoms is $\sim 20{,}000$ m/sec, about twice as fast as neutral carbons. Therefore, a possible conclusion is that some of the C_{II} atoms created early in the discharge recombine to neutral carbon and exit at 18,000 m/sec. This velocity is well in excess of the bulk of the neutrals which are created later in the discharge when the energy left in the capacitor is too small for ionization. These neutrals will move more slowly because there is relatively less energy available to push (via collisions) the neutrals out. This tends to confirm our suspicions that the discharge is initially highly ionized and that most neutrals are created after the energy available to ionize them has been dissipated.

One of the important open questions about this thruster is whether the thrust is the result of magnetic pressure on the ionized species or gas dynamic pressure on the neutrals. In other words, is the total momentum of the exhaust given by the mass of the charged species times their (relatively high) velocity, or by the neutral mass and velocity? To try to resolve this question we measured the velocity associated with each line by a Doppler technique.

The apparatus used to view the light end on (down the thrust axis) and perpendicular to the axis is shown in Fig. 2a. Two separate light tubes, one terminated in a 45° mirror, extend into the discharge an inch in front of the Teflon face and in line with the exhaust. The light from these tubes is fed alternately to the spectrometer by gating open each channel with a slotted wheel. This wheel triggers two microswitches a total of four times on each revolution. The first steers the photodiode signal to a boxcar integrator and the second initiates the discharge. On the next half-revolution the third

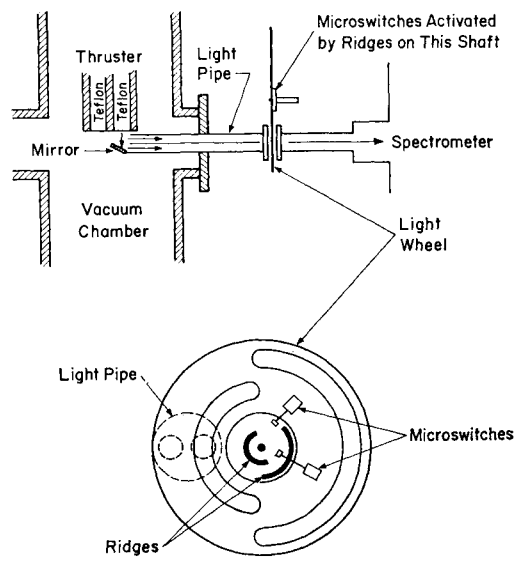

Fig. 2a Arrangement for alternating the side-on and end-on light from the discharge on the spectrometer.

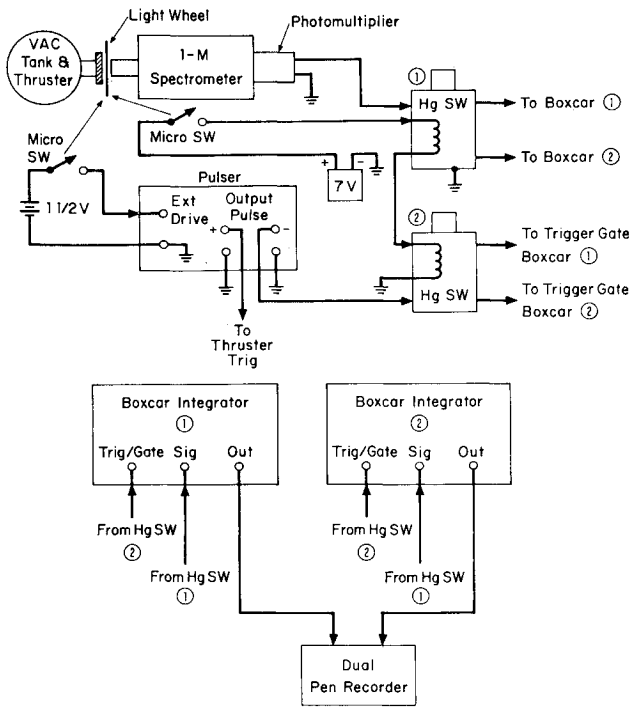

Fig. 2b Switching arrangement for sending alternate light signals to different boxcar integrators.

trigger steers the output to the second boxcar integrator and the fourth initiates the discharge again. The circuitry is shown on block diagram form in Fig. 2b. The line being observed is scanned very slowly (0.5 Å/min over a 60 sec period) and the intensity in any particular wavelength slice $\Delta\lambda$ (which is small compared to the line width) is the average over many pulses. To complete the setup, the output from the two light channels are displayed simultaneously on a dual-trace recorder for direct measurement of the Doppler shift.

The result for a particular line F_I at 6902 Å is shown in Fig. 3. The shift there (0.13 Å) corresponds to a velocity of 5650 m/sec. Note that the line widths are large compared to the line shift, so our accuracy is not very good. Another contributor to poor accuracy is the statistical fluctuation from shot to shot. This is overcome in part by using the boxcar integrator, but there is a maximum repetition rate for the thruster, a maximum time between pulses to leave the charge stored on the boxcar, a minimum drive speed on the scanning spectrometer, and a maximum "gate open" time to look at the

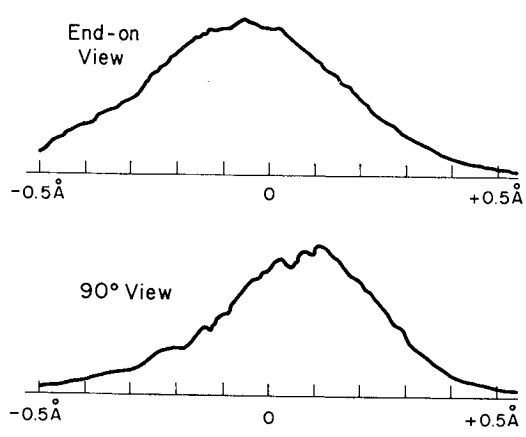

Fig. 3 Perpendicular and end-on views of the neutral fluorine line at 6902 Å showing a Doppler shift of —0.13 Å corresponding to a velocity 5650 m/sec.

Table 2 Carbon and Fluorine Velocities

Species	Wavelength (Å)	Energy level (ev)	Velocity by Doppler shift (m/sec)	Velocity by time of flight (m/sec)
C_I	2479	7.7	11,000	6,000
	2583	7.5	16,000	18,000
C_{II}	2993	22.2	11,000	25,000
	6578	16.3	...	28,000
C_{III}	2297	18.1	13,000	...
	4187	43.0	16,000	...
	4647	32.2	...	28,000
	4650	32.2	...	42,000
C_{IV}	2405	55.8	21,000	...
	2530	55.8	27,000	36,000
	4658	58.4	35,000	32,000
F_I	6856	14.5	4,000	12,000
	6902	14.5	6,000	11,000
F_{II}	3501	28.7	5,000	18,000
	4246	31.6	...	20,000
F_{III}	2760	47.1	14,000	...
	3043	46.7	12,000	28,000
	3175	44.2	...	23,000
F_{IV}	2171	58.2	22,000	...
	2826	56.1	22,000	36,000

light. All of these combine to make this measurement difficult. On some lines the uncertainty is at least a factor of two because the Doppler shift is less than 20% of the full line width and the line profiles are not smooth.

Nonetheless, a summary of the velocity obtained in this way for each line is given in Table 2. Before commenting on the results, note that the last column gives the velocity as measured by an optical time-of-flight technique. Here we simply observed the time of peak light intensity for each line as the thruster is moved from one to three inches away from the light path (now viewing from the side only). The time-of-flight data give consistently higher velocities than the Doppler for reasons we cannot explain.

The average of both methods for all lines of a particular species is given in Table 3. The salient feature of this presentation is that the more highly ionized the species, the higher is its velocity. Such a result is not at all unreasonable, but it does prove that the exhaust is a rather complex mixture of ions and neutrals.

The variation is due in part to measurement errors and in part to variations in velocities among different lines of the same species. The latter variation has already been noted between the 2479 Å and 2583 Å C_I lines. A similar distinction could probably be made among different lines of the same species in Table 2, because some of the C_{II} lines for instance could be the result of recombination of C_{III} with an electron. That line would then have a velocity closer to the average C_{III} velocity than to the average C_{II} velocity.

Table 3 Average velocity ranges for the various species of carbon and fluorine

Species	Velocity (m/sec)	Species	Velocity (m/sec)
C_I	5,000–15,000	F_I	5,000–15,000
C_{II}	20,000–30,000	F_{II}	15,000–25,000
C_{III}	30,000–40,000	F_{III}	25,000–35,000
C_{IV}		F_{IV}	

A final observation concerns the line broadening. Almost all lines have a half-width of ~0.25 Å, which corresponds to an ion temperature of 12 ev if the mechanism was Doppler broadening by thermal motion. However, at these densities (estimated at $\sim 10^{16}/cm^3$ or higher) Stark broadening is possible. Further conclusions must await better density measurements.

Faraday Cup Measurements

One of the numbers which would help to determine the thrust contributed by fast ions is the percentage of ionization. To measure that we integrated the ion current to the Faraday cup as we scanned across the exhaust perpendicular to the thrust axis. By scanning horizontally and vertically we found profile of the exhaust plume. and from the geometry of the collector (hole size, orientation, distance to Teflon, etc.) calculated the total charge in the exhaust. Each shot ablates 10^{-8}Kg of C_2F_4 which means 6×10^{16} molecules (3.6×10^{17} atoms of C,F). The total charge was 5.23×10^{-3} coulomb, equivalent to 3.28×10^{16} singly ionized particles. There are multiply ionized species of course, and since we do not know the fractional breakdown of the total number of ions, we cannot say how many total particles this really is. However, if they were singly ionized the gas would be 10% ionized.

The charge collected by the cup on axis as a function of distance along the axis is found by integrating the collected current in time. Theoretically, if the previous assumption of a drifting Maxwellian created at a point at $t = 0$ were correct, the charge should be proportional to $1/L^2$. This behavior is confirmed by Fig. 4. (The peak current to the cup varies as $1/L^3$.)

Conclusions

From the measurements reported here we can construct a model of the formation and acceleration of the exhaust particles. According to Table 1, the triply ionized particles are created first, indicating that there is an excess of avialable energy in the initial ionizing current. Thus, the first Teflon molecules which are ablated are dissociated and multiply ionized.

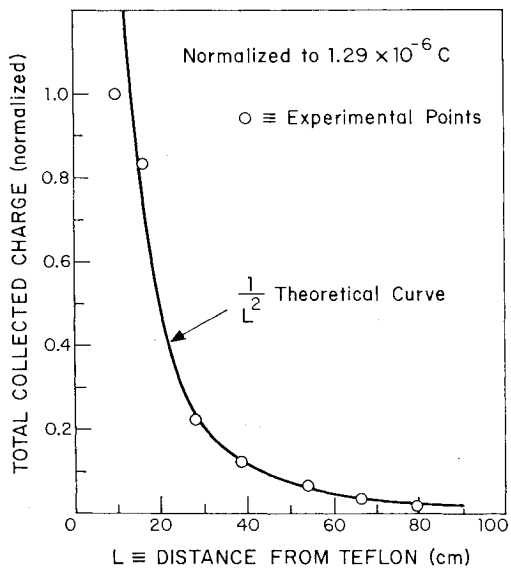

Fig. 4 Charge collected by a Faraday cup vs distance from the source.

With this initial increase of plasma density, the primary ionizing electrons begin colliding more often, presumably slowing down so that only doubly ionized species can then form. Further plasma formation allows only singly ionized species. Eventually, there is insufficient energy to ionize the atoms, hence there are only excited neutrals being formed.

It is important to note that ablation energies are low and since there is a rather long lasting (5 μsec) hot plasma (~10 ev) there is a continual production of molecules from the Teflon fuel long after the capacitor energy is expended. This we believe leads to the poor mass utilization quoted earlier. The preceding picture assumes distinct formation times for the various species, consistent with observations. This is also consistent with the fact that the momentum transfer rates in the plasma are so high at the densities and temperatures in the arc (10^{16} @10 ev) that if all the ions were created at the same time their velocities would quickly equilibrate.

From the measurement of total charge collected by the Faraday cup we estimate that more than 90% of the exhaust is made up of neutral atoms and molecules, these presumably being ablated by thermal bombardment of the Teflon surface by hot plasma particles after the capacitor energy is expended. These neutrals probably have negligible velocities because all ions and excited atoms have velocities in excess of the mass-averaged velocity. Furthermore, the total exhaust momentum can be accounted for by the fast ions, estimating their total mass from the charge measurement. A more accurate partitioning requires mass measurements of the individual species.

It is clear from the preceding picture that considerably more energy is given to the exhaust to produce its momentum than would be the case if all ablated atoms were accelerated to the same exit velocity. However, based on this model several remedies are suggested. First, to prevent dumping excessive energy into multiple ionization owing to an initial fuel starvation we altered the fuel feed, hopefully to enable more ablated particles to get into the throat more quickly. This was done by feeding fuel from both sides of the throat rather than from the back. An optimum (close) spacing was found which maximizes the thrust but ablates even more fuel. Nontheless, this does increase the product $I_{SP}I_{bit}$. Second, by altering the geometry of the return current path to minimize the inductance and maximize the magnetic pressure on the arc, one can force the arc off the fuel surface more quickly. This configuration (without side feed) results in a three-fold increase in I_{SP} at $\frac{5}{7}$ the thrust level. Combinations of these techniques can be used to improve the thruster performance.

References

[1] Guman, W. J., and Peko, P. E., "Solid Propellant Pulsed Plasma Microthruster Studies," *Journal of Spacecraft and Rockets*, Vol. 5, No. 6, June 1968, pp. 732–733.

[2] Maclellan, D. C., MacDonald, H. A., Waldron, P., and Sherman, H., "Lincoln Experimental Satellites 5 and 6," AIAA Paper 70-494, Los Angeles, Calif., 1970.

[3] Guman, W. J., and Nathanson, D. M., "Pulsed Plasma Microthruster Propulsion System for Synchronous Orbit Satellite," *Journal of Spacecraft and Rockets*, Vol. 7, No. 4, April 1970, p. 409.

[4] Vondra, R., Thomassen, K., and Solbes, A., "Analysis of Solid Teflon Pulsed Plasma Thruster," *Journal of Spacecraft and Rockets*, Vol. 7, No. 12, Dec. 1970, p. 1403.

[5] Vondra, R., Thomassen, K., and Solbes, A., "A Pulsed Electric Thruster for Satellite Control," *Proceedings of IEEE*, Vol. 59, No. 2, pp. 271–277.

[6] Malliaris, A. C. and Libby, B. R., "Spectroscopic Study of an Ion–Neutral Coupling in Plasma Acceleration," *AIAA Journal*, Vol. 9, No. 1, Jan. 1971, pp. 160–167.

[7] Striganov, A. R. and Sventitskii, N. S., "Tables of Spectral Lines of Neutral and Ionized Atoms," IFI/Plenum, New York–Washington 1968.